A realistic simulation framework for assessing deformable slice-to-volume (CT-fluoroscopy/CT) registration

Ziv Yaniv[a], Roland Stenzel[a,b], Kevin Cleary[a], and Filip Banovac[a,c]

[a]Imaging Science and Information Systems (ISIS) Center, Dept. of Radiology, Georgetown University Medical Center, Washington, DC,USA
[b]University of Karlsruhe, Institut für Technische Informatik - IAIM, Karlsruhe, Germany
[c]Georgetown University Hospital, MedStar Health, Washington, DC, USA

ABSTRACT

Lung cancer screening for early diagnosis is a clinically important problem. One screening method is to test tissue samples obtained from CT-fluoroscopy (CTF) guided lung biopsy. CTF provides real-time imaging; however on most machines the view is limited to a single slice. Mentally reconstructing the direction of the needle when it is not in the imaging plane is a difficult task. We are currently developing 3D visualization software that will augment the physician's ability to perform this task. At the beginning of the procedure a CT scan is acquired at breath-hold. The physician then specifies an entry point and a target point on the CT. As the procedure advances the physician acquires a CTF image, at breath-hold; the system then registers the current setup to the CT scan, enabling comparison between the plan and current situation. As the CT and CTF data are acquired at different breath-holds we expect them to exhibit displacements of up to 4mm. To assess the performance of different registration algorithms for CTF/CT registration we propose to use simulated CTF images. These images are created by deforming the original CT volume and extracting a slice from it. Realistic deformation of the CT volume is achieved by using positional information from electromagnetically tracked fiducials, acquired throughout the respiratory cycle. To estimate the dense displacement field underlying the sparse displacement field provided by the fiducials we use radial basis function interpolation. Finally, we evaluated Thirion's "demons" algorithm, as implemented in ITK, for the task of slice-to-volume registration. We found it to be unsuitable for this task, as in most cases the recovered displacements were less than 50% of the original ones.

Keywords: Image-Guided Therapy, CT-Fluoroscopy, deformable registration, simulated respiration, radial basis functions

1. INTRODUCTION

Lung cancer is a leading cause of death in the United States with an overall cure rate (five year survival) of only about 15%.[1] Lung cancer screening has the potential of leading to early diagnosis and treatment, thus increasing chances of survival.[2] One screening method is to test tissue samples obtained from CT-Fluoroscopy (CTF) guided lung biopsy.

The outcome of this approach is highly dependent on the ability of the physician to accurately place the biopsy needle within the suspected nodule based on the CTF images. CTF provides the physician with real-time imaging, however on most machines it is limited to a single slice. Mentally reconstructing the direction of the needle, when it is not in the imaging plane, using a single slice as feedback can be a difficult task, even for experienced physicians.

We are currently developing 3D visualization software that may augment the physician's ability to perform this task. The system works as follows. At the beginning of the procedure a CT scan is acquired at breath-hold. The physician then specifies an entry point and a target point on the CT. As the procedure advances, the physician acquires a CTF image at breath-hold; the system then registers the current setup to the CT scan, enabling comparison between the plan and current situation. As the CT and CTF data are acquired at different breath-holds we need to deformably register them.

E-mail: {zivy,stenzel,cleary}@isis.georgetown.edu

As the whole system depends on accurate CTF/CT registration we first need to evaluate the performance and limitations of different deformable registration algorithms. We propose to use a simulation framework for respiratory based motion, allowing us to validate registration results with regard to a known transformation. To simulate a CTF image we extract a slice from a second volumetric data set whose transformation with regard to the original volume is known. Three possible methods to obtain a second volumetric data set with known deformations are: (1) Ad-hoc methods; (2) Registration based methods; and (3) Finite element methods (FEM).

Ad-hoc methods receive as input a volumetric data set and a sparse displacement field describing the deformation. They output a dense displacement field and a corresponding deformed volume. The sparse displacement field is generated by manually displacing a small number of points. The points are usually anatomical landmarks with the displacement field generated via interpolation[3] or approximation.[4] Points may also be the intersections of a regular grid that overlaps the image with the displacement field generated via free-form deformations.[5] The popularity of this approach is due to its simplicity, and that it does not require additional data (i.e. only the original volume is required). Unfortunately, as the approach is not constrained, physically impossible deformations are easily generated.

Registration based methods receive as input multiple volumetric data sets under different deformations. They output a dense displacement field describing the deformation between pairs of volumes.[6,7] This approach does not incorporate bio-mechanical knowledge, but works well if the deformation between the registered data sets is smooth. Applying this approach to structures that deform considerably requires acquisition of multiple data sets throughout the deformation process (e.g. a set of MRI volumes acquired between end expiration and end inspiration). Note that using the displacement field generated by this approach as a gold standard can be biased if the same algorithm is used for volume-to-volume and slice-to-volume registrations.

Finite element methods receive as input a volumetric data set, a segmentation of the anatomical structures according to the different tissue types, and the bio-mechanical properties of the tissue types. They output a dense displacement field and a corresponding deformed volume. These methods have have been studied extensively, mainly in the context of surgical simulation,[8,9] and registration.[10,11] This approach is considered the most physically accurate, and has been used to validate free-form registration of mammographic MRI data.[12]

Our approach to simulating deformation due to respiratory motion can be classified as a constrained version of the ad-hoc approach. We deform the original volumetric data based on the motion of a sparse set of points, electromagnetically tracked fiducials, which are acquired from organ motion of a respiring animal. As is the case with the ad-hoc approach, computing the deformation is still an under-constrained problem. The difference is that now the deformations are driven by physical measurements and not arbitrary displacements. Figure 1 classifies the different approaches according to their computational complexity and physical realism.

Similar approaches to our own have been recently described in the context of real-time deformation update of a CT volume.[13,14] Both papers estimate deformations of small volumes using electromagnetically tracked fiducials. In[13] the deformation field is obtained using a variational approach, with a regularization term that enforces smoothness. No quantitative results are given and the weighing of the regularization term is unspecified. In[14] the deformation is assumed to be affine which is plausible for very small volumes.

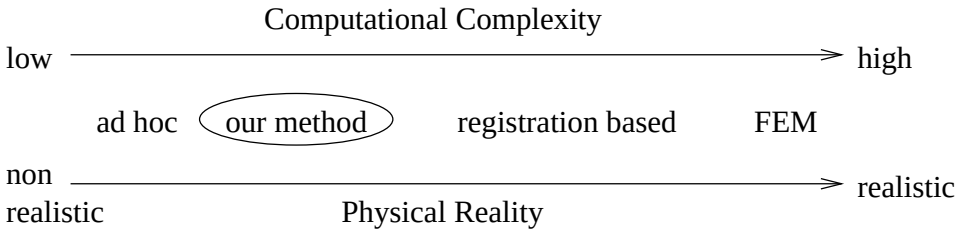

Figure 1. Classification of approaches for creating a ground truth displacement field and deformed volumetric data set.

2. MATERIALS AND METHODS

To assess the accuracy of deformable slice-to-volume (CTF/CT) registration we have developed a simulation based framework for respiratory based motion, providing a ground truth to which registration results can be compared. Our method is based on simulating CTF images using a CT scan acquired at end expiration that is deformed according to data obtained from electromagnetically tracked fiducials.

2.1. Data simulation

Simulating CTF images at different stages of the respiratory cycle is a four step process: (1) Acquire a CT scan and positional information from electromagnetically tracked fiducials; (2) Compute a deformation field based on the electromagnetic tracking data, and segment the lung region in the CT. (3) Deform the original volume in the region of the lungs using the segmentation and deformation field from the previous step. (4) Extract a slice from the deformed volume, this is our simulated CTF image.

Data acquisition proceeds as follows. First, four magnetically tracked fiducials are placed in the animal's liver (Fig. 2(a)), under an approved protocol, and a CT is acquired at end expiration. Then the animal is transferred to an environment where there are no ferromagnetic materials and positional data from the fiducials is acquired throughout several respiratory cycles. CT acquisition is performed at end expiration to ensure that there are no motion artifacts during imaging. In our setup the animal is on a respirator and we allow its lungs to deflate prior to imaging. The needles were placed in the liver instead of the lungs, as placing them in the lungs may result in a pneumothorax (Fig. 2(b)). This is a condition where air collects in the space surrounding the lungs causing them to collapse.

Deformation field computation is based on the known motion of fiducials inside the volume. This data is used to estimate the motion of all points in the volume, using radial basis function interpolation. As a pre-processing step we need to orient the electromagnetic system's coordinate frame with the CT coordinate frame (Fig. 2(c)). When three or more needles are used we compute the orientation using rigid registration.[15] If less than three needles are used we obtain the orientation by analyzing their motion pattern using principle component analysis. We transform the motion data to the coordinate system defined by the principle components and identify the main direction of motion with the CT's z axis (cranial-caudal), and the direction with least motion with the CT's x axis (left-right). This identification is based on the assumption that maximal motion is in the cranial-caudal direction and least motion is in the left-right direction. Finally, the initial positions of the needles are translated so that they are inside the lung region.

Once the data is oriented and translated we have the motion of the tracked fiducials, in the CT coordinate system, throughout the respiratory cycle. For different points in time we have corresponding vectors specifying the fiducial displacement from its initial location. This allows us to compute deformation fields corresponding to different points in the respiratory cycle. The fields are computed using radial basis functions with the input being the original point locations, and corresponding displacements.

In general the radial basis function interpolator is of the form:

$$s(\mathbf{x}) = p(\mathbf{x}) + \sum_{i=1}^{n} \lambda_i \phi(\|\mathbf{x} - \mathbf{x_i}\|)$$

where $p(\mathbf{x})$ is a polynomial that ensures the invertibility of the associated set of linear equations, λ_i are real coefficients, $\phi : \mathbb{R}^+ \to \mathbb{R}$ is the basis function, and $\mathbf{x_i} \in \mathbb{R}^d$ are the interpolation points such that $s(\mathbf{x_i}) = f_i$. In our case $\mathbf{x_i}$ are the fiducial locations at end expiration, and f_i are the corresponding translations in the x, y and z directions.

The radial basis function we use is a Gaussian, $\phi(r) = e^{-cr^2}, c > 0$, as it guarantees the existence of a solution without any restrictions on the spatial location of the known points.[16] This eliminates the need for the polynomial term $p(\mathbf{x})$ giving a linear equation system with a symmetric positive definite matrix $A_{ij} = \phi(\|\mathbf{x_i} - \mathbf{x_j}\|)$:

$$A \begin{bmatrix} \lambda_1 \\ \vdots \\ \lambda_n \end{bmatrix} = \begin{bmatrix} f_1 \\ \vdots \\ f_n \end{bmatrix}$$

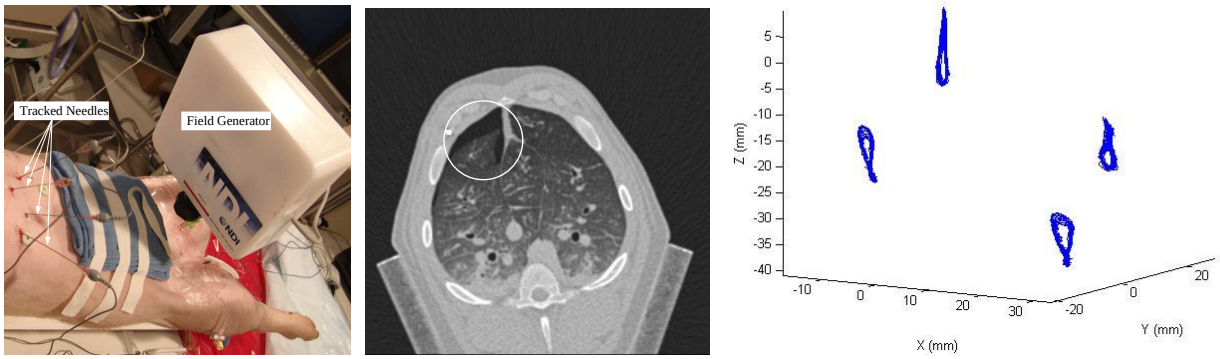

(a) (b) (c)

Figure 2. Electromagnetic tracking data acquisition: (a) needles placed in animals' liver; (b) circle marks pneumothorax caused by a needle inserted into the animal's lung; and (c) tracking data acquired throughout several breathing cycles oriented to the CT coordinate system (x axis is left-right, y axis is anterior-posterior, and z axis is cranial-caudal).

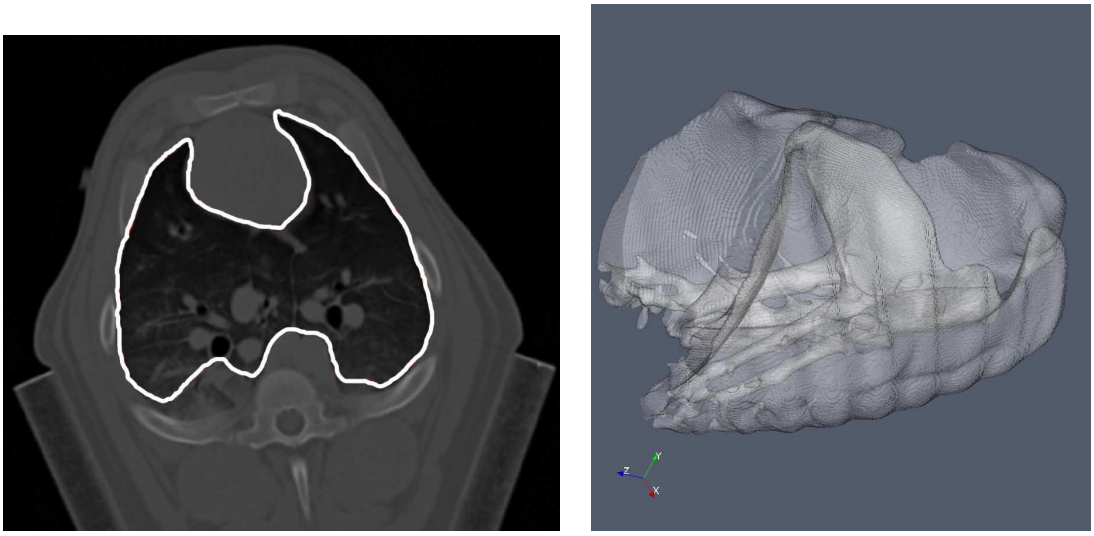

(a) (b)

Figure 3. Segmentation of lung region from CT data set (a) slice and (b) volume rendering of segmented region.

Generally, the use of radial basis functions with infinite support is viewed as a deficiency, as each interpolation point influences the function approximation at all locations. In our case, as we are dealing with a very small number of interpolation points, we do want them to effect the function evaluation throughout the volume. By choosing a Gaussian as our basis function each interpolation point effects the whole volume while at the same time its influence diminishes as a function of the distance.

This most likely yields an inaccurate approximation of the underlying function, mainly due to the spatial sparseness of the sampling, but it is still plausible as assessed by visual inspection. Additionally deformation sizes are limited to reasonable ones. This is achieved by empirically setting the Gaussian's standard deviation to values such that the estimated motion is smaller than 1.5 times the maximal known motion from electromagnetic tracking.

Finally, as we are only interested in the region of the lungs we segment them both in the CTF and CT images so that the resulting images include only the region of interest. The deformation field is then limited to this region. Segmentation of the lungs is done by first blurring the images using a Gaussian kernel with a standard

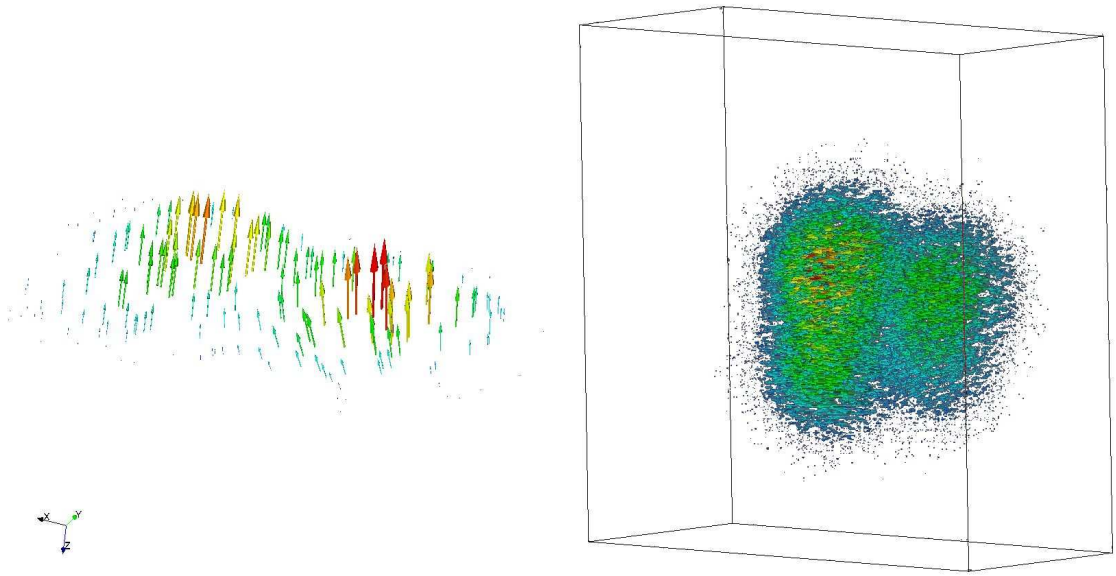

(a) (b)

Figure 4. Deformation field limited to region of the lungs (a) single slice, and (b) whole field.

deviation of $2mm$, and then applying a threshold based region growing method. Seed points are placed in the left and right lungs and all voxels whose intensity is less than the threshold (0 HU) are considered as part of the lung. This approach is viable, as there is a clear intensity boundary between the lungs and the surrounding tissue (Fig. 3). In our case, segmentation accuracy is not an issue, as the results are only used as a region of interest. Fig. 4 is an example of the final deformation field limited to the region of the lung.

3. EXPERIMENTAL RESULTS

In all experiments CT images were acquired using a Siemens Somatom Volume Zoom machine, with slice resolution of 512X512 and pixel spacing of $0.61\text{X}0.61mm$ and $1mm$ slice spacing. Electromagnetic data was acquired using MagTrax needles from Traxtal Technologies (Belaire, Texas, USA), and the Aurora electromagnetic tracking system from Northern Digital Inc. (Ontario, Canada). Acquisition rate of the tracking data was 25Hz.

CT and electromagnetic data were acquired in two swine animal studies, under an approved protocol, and used to simulate seven CTF images per data set. As both the CT and CTF images are acquired with similar breath-holds, we expect the two acquisitions will exhibit small deformations of up to $4mm$. Simulated CTF images were generated accordingly, with deformations in the range 0.4–$4.2mm$.

The CT data and simulated images were then used to assess the capabilities of Thirion's "demons" algorithm,[17] as implemented in ITK,[18] to perform slice-to-volume deformable registration. This algorithm is an optical flow based method, most notably it assumes that the constant brightness constraint[19] is satisfied, that is, a point's intensity does not change between images. In the case of CTF/CT registration this assumption is indeed satisfied.

Two factors that can effect the convergence range of the registration process are its initialization, and the size of the displacements that we are trying to recover. In our case CT and CTF images are different modes of operation of the same machine, so their coordinate systems are intrinsically aligned. This allows us to use the slice location of the CTF image as our initial transformation, an approach we also apply in our simulation studies. The size of the displacements we are trying to recover is relatively small, less than $4mm$, but it varies with the slice location in the lung. To assess the effect of slice location, for each simulated deformation we registered four slices from lung apex to diaphragm, as shown in Figure 5.

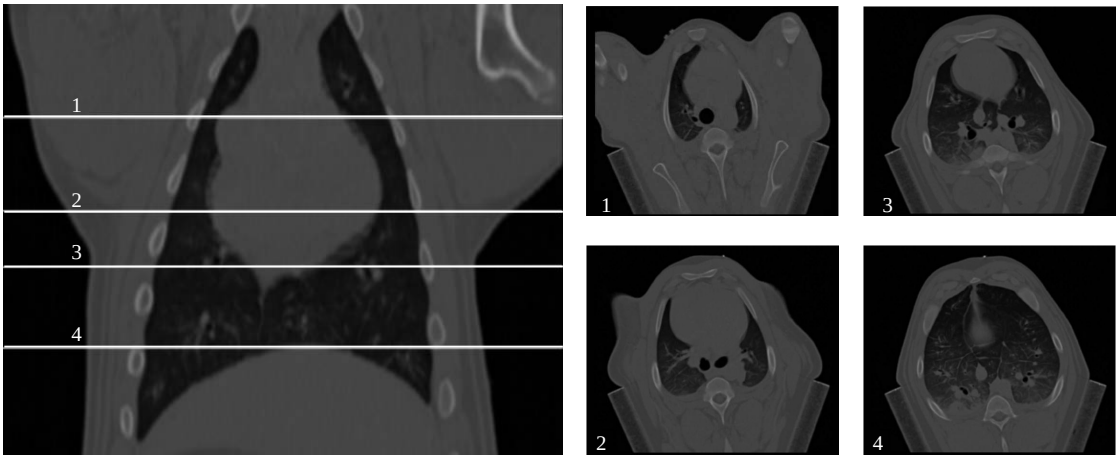

Figure 5. To assess the registration performance for different regions of the lung we register four different slices from apex (1) to diaphragm (4).

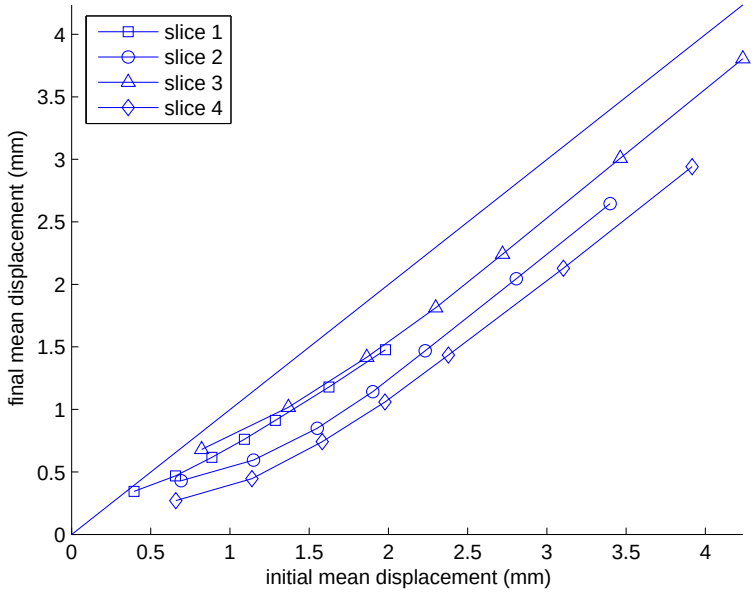

Figure 6. Registration results using slices from different locations in the lung. Slices correspond to those in Fig. 5, and are ordered from apex (1) to diaphragm (4). Results are below the diagonal, indicating that the algorithm was able to reduce the original displacements. However, the accuracy of the final results is not sufficient for our application.

In all our experiments the "demons" algorithm failed to converge to the global optimum. The results of our experiments are summarized in Figure 6. In all experiments the algorithm was able to reduce the initial displacements, results are below the diagonal indicating decrease in the mean displacement. Unfortunately, in most cases the final recovered displacements are less than 50% of the original ones.

4. DISCUSSION AND CONCLUSIONS

We have presented a simple method for simulating soft tissue deformation. The method estimates the deformation based on a small set of landmarks whose displacement is precisely known. Although the resulting deformations

are not physically accurate, they are still plausible ones, and are generally more accurate than deformations generated by manual methods.

In this work positional data of internal points was obtained via electromagnetic tracking. In general, our approach does not require an electromagnetic tracking system. Other options include the use of rigid needles and optical tracking, or the use of fiducials and bi-plane fluoroscopy to track internal organ motion throughout the respiratory cycle.[20]

Finally, we have assessed the performance of Thirion's "demons" algorithm, as implemented in ITK, for slice-to-volume registration using our simulation framework. According to our experiments using this algorithm for deformable slice-to-volume registration does not yield satisfactory results.

Although deformable slice-to-volume is an ill posed problem we initially expected the "demons" algorithm would be able to recover the correct displacements as they are relatively small (less than $4mm$). Given our results we will investigate the possibility of acquiring multiple (two or three) CTF images at different slice positions instead of a single CTF image. This will change our registration approach from slice-to-volume to volume-to-volume. As the volume-to-volume approach incorporates more information it is better conditioned and has a better chance of recovering the correct deformations.

ACKNOWLEDGMENTS

This work was funded by U.S. Army grants DAMD17-99-1-9022 and W81XWH-04-1-0078. The content of this manuscript does not necessarily reflect the position or policy of the U.S. Government.

REFERENCES

1. "American cancer society: Cancer facts and figures," 2004.
2. O. S. Miettinen, "Screening for lung cancer," *Radiol. Clin. North. Am.* **38**(3), pp. 479–486, 2000.
3. F. L. Bookstein, "Principal warps: Thin-plate splines and the decomposition of deformations.," *IEEE Trans. Pattern Anal. Machine Intell.* **11**(6), pp. 567–585, 1989.
4. K. Rohr, H. S. Stiehl, R. Sprengel, T. M. Buzug, J. Weese, and M. H. Kuhn, "Landmark-based elastic registration using approximating thin-plate splines.," *IEEE Trans. Med. Imag.* **20**(6), pp. 526–534, 2001.
5. D. Rueckert, L. I. Sonoda, C. Hayes, D. L. G. Hill, M. O. Leach, and D. J. Hawkes, "Non-rigid registration using free-form deformations: Application to breast MR images.," *IEEE Trans. Med. Imag.* **18**(8), pp. 712–721, 1999.
6. D. J. Hawkes *et al.*, "Tissue deformation and shape models in image-guided interventions: a discussion paper," *Medical Image Analysis* **9**(2), pp. 163–175, 2005.
7. T. Rohlfing, C. Maurer, Jr., W. G. O'Dell, and J. Zhong, "Modeling liver motion and deformation during the respiratory cycle using intensity-based free-form registration of gated MR images," *Medical Physics* **31**(3), pp. 427–432, 2004.
8. H. Delingette, "Towards realistic soft tissue modeling in medical simulation," *Proceedings of the IEEE : Special Issue on Surgery Simulation* , pp. 512–523, 1998.
9. J.-M. Schwartz, M. Denninger, D. Rancourt, C. Moisan, and D. Laurendeau, "Modelling liver tissue properties using a non-linear visco-elastic model for surgery simulation," *Medical Image Analysis* **9**(2), pp. 103–112, 2005.
10. K. E. Lunn, K. D. Paulsen, D. W. Roberts, F. E. Kennedy, A. Hartov, and L. A. Platenik, "Nonrigid brain registration: synthesizing full volume deformation fields from model basis solutions constrained by partial volume intraoperative data," *Computer Vision and Image Understanding* **89**, pp. 299–317, 2003.
11. M. Ferrant, S. K. Warfield, A. Nabavi, F. A. Jolesz, and R. Kikinis, "Registration of 3d intraoperative MR images of the brain using a finite element biomechanical model.," in *Medical Image Computing and Computer-Assisted Intervention*, pp. 19–28, 2000.
12. J. A. Schnabel, C. Tanner, A. D. Castellano-Smith, A. Degenhard, M. O. Leach, D. R. Hose, D. L. G. Hill, and D. J. Hawkes, "Validation of non-rigid image registration using finite element methods: Application to breast MR images.," *IEEE Trans. Med. Imag.* **22**(2), pp. 238–247, 2003.

13. M. Vetter *et al.*, "Navigation aids and real-time deformation modeling for open liver surgery," in *SPIE Medical Imaging: Visualization, Image-Guided Procedures, and Display*, pp. 58–68, 2003.
14. H. Zhang, F. Banovac, N. Glossop, and K. Cleary, "Two-stage registration for real-time deformable compensation using an electromagnetic tracking device," in *Medical Image Computing and Computer-Assisted Intervention*, pp. 992–999, 2005.
15. B. K. P. Horn, "Closed-form solution of absolute orientation using unit quaternions," *Journal of the Optical Society of America A* **4**(4), pp. 629–642, 1987.
16. M. J. D. Powell, "The theory of radial basis function approximation in 1990," in *Advances in Numerical Analysis Volume II: Wavelets, Subdivision Algorithms and Radial Basis Functions*, W. A. Light, ed., Oxford University Press, 1992.
17. J. P. Thirion, "Image matching as a diffusion process: an analogy with maxwell's demons," *Medical Image Analysis* **2**(3), pp. 243–260, 1998.
18. L. Ibáñez, W. Schroeder, L. Ng, and J. Cates, *The ITK Software Guide*, Kitware Inc., 2005.
19. B. K. P. Horn and B. G. Schunck, "Determining optical flow," *Artificial Intelligence* **17**(1–3), pp. 185–203, 1981.
20. Z. Yaniv and K. Cleary, "Fluoroscopy based accuracy assessment of electromagnetic tracking," in *SPIE Medical Imaging: Visualization, Image-Guided Procedures, and Display*, 2006.